

**Al-Mg ISOTOPIC CONSTRAINTS ON ALTERATION OF ALLENDE Ca-AL-RICH INCLUSIONS.** T. J. Fagan<sup>1</sup>, Y. Guan<sup>2</sup> and G. J. MacPherson<sup>3</sup>, <sup>1</sup>Waseda University, Geology Department, 1-6-1 Nishiwaseda, Shinjuku, Tokyo, 169-8050, Japan (fagan@waseda.jp), <sup>2</sup>Department of Geological Sciences, Arizona State University, Tempe, AZ 85287, USA. National Museum of Natural History, Smithsonian Institution, Washington, DC 20560, USA.

**Introduction:** Ca-Al-rich inclusions (CAIs) from the Allende CV3 chondrite show textures indicating that melilite and to some extent, primary anorthite were partially replaced by secondary minerals, including grossular, monticellite, secondary anorthite and feldspathoids [1-4]. Whether these secondary minerals originated during one or multiple stages of alteration, and in a nebular or asteroidal setting or both, have implications for nebular history and alteration processes. This study is a continuation of our efforts to address this issue using Al-Mg isotope systematics to evaluate the timing of alteration.

**Analytical Methods:** Polished thin sections of two Allende CAIs, USNM 4022-1 and USNM 3529-47-1, were characterized using a petrographic microscope and a JEOL JSM-840A scanning electron microscope (SEM). Elemental compositions were measured with both energy dispersive (on the SEM) and wavelength dispersive techniques (using a JEOL JXA-8900 electron microprobe).

Isotopic measurements were collected using the ASU Cameca ims-6f ion microprobe. A 12.5 kV O<sup>-</sup> primary beam of 0.05 – 0.2 nA was focused into a <5 μm spot for all analyses. Secondary ions were accelerated to 10 kV and collected with an energy band-pass of ~50 V under a mass resolving power of ~3500.

**Mineralogy and Textures:** CAI 4022-1 is a type B2 CAI with coarse-grained primary melilite, anorthite, Ca-Ti-pyroxene (fassaite) and Mg-spinel, and an incomplete Wark-Lovering (WL) rim dominated by diopside. A narrow zone inside of the WL diopside is dominated by fine-grained feldspathoid, Fe-bearing spinel, and thin laths of secondary anorthite. Feldspathoid-rich patches also occur in the interior of the CAI (Fig. 1A), where the secondary anorthite is coarser and more equant than the lath-shaped anorthite near the CAI rim. Melilite and primary anorthite throughout the CAI are transected and bounded by alteration veins dominated by grossular with some monticellite or secondary anorthite (Fig. 1A).

CAI 3529-47-1 is a fluffy type A CAI composed of numerous individual nodules enclosed in and partially separated from one another by meteorite matrix and accretionary rim material. Melilite is the dominant primary mineral in the nodules, with accessory spinel and perovskite; diopside forms a thin rim around each nodule (Fig. 1B). All of the

nodules show some replacement of primary melilite by fine-grained secondary lath-like anorthite, feldspathoids, grossular, and Fe-bearing spinel (Fig. 1B).

**Al-Mg Isotopic Results:** Some analyses of primary anorthite from CAI 4022-1 have <sup>26</sup>Mg excesses indicating “canonical” [5] initial <sup>26</sup>Al/<sup>27</sup>Al ratios (Fig. 2A); however, several analyses, particularly those with high Al/Mg ratios, form a spread with lower relative <sup>26</sup>Mg excesses. We infer that this deviation from canonical is caused primarily by partial re-equilibration after initial crystallization (e.g., [6]). In addition to these results, one analysis of primary anorthite with exceptionally high Al/Mg (~1050) exhibits no <sup>26</sup>Mg excess.

All analyses of secondary anorthite from 4022-1 show no excesses of <sup>26</sup>Mg (Fig. 2A). The other secondary phases have lower Al/Mg; however, resolvable excess <sup>26</sup>Mg (<sup>26</sup>Mg/<sup>24</sup>Mg = 0.1403 ± 0.0003, <sup>27</sup>Al/<sup>24</sup>Mg = 29.6 ± 0.9, initial <sup>26</sup>Al/<sup>27</sup>Al ~ 3 × 10<sup>-5</sup>; uncertainties reported throughout are 2σ) was detected in one of three grossular grains analyzed.

Analyses of gehlenitic melilite from fluffy type A CAI 3529-47-1 show canonical Al-Mg isotopic systematics (Fig. 2B). Except for one analysis of sodalite (<sup>26</sup>Mg/<sup>24</sup>Mg = 0.139 ± 0.003, <sup>27</sup>Al/<sup>24</sup>Mg = 2200 ± 100) and one of anorthite (<sup>26</sup>Mg/<sup>24</sup>Mg = 0.1388 ± 0.0004, <sup>27</sup>Al/<sup>24</sup>Mg = 31.8 ± 1.6), our results from secondary anorthite, grossular and feldspathoids from this CAI have <sup>26</sup>Mg excesses that correlate with Al/Mg (Fig. 2C). A regression through these points (excluding the sodalite and anorthite noted above) yields initial <sup>26</sup>Al/<sup>27</sup>Al of 4.7 (± 2.6) × 10<sup>-6</sup> with initial <sup>26</sup>Mg/<sup>24</sup>Mg = 0.13985 ± 0.00020 (MSWD = 0.74).

**Timing and Setting of Alteration Events:** These analyses combined with our initial results from a type B2 and a compact type A CAI [4] suggest complex alteration histories for Allende CAIs. Most of the secondary phases from the three compact CAIs investigated show no excesses of <sup>26</sup>Mg, consistent with late (parent-body setting) alteration. However, some grossular analyses have significant <sup>26</sup>Mg excesses, as do nearly all the secondary phases analyzed from a fluffy type A CAI. If the Al-Mg system can be applied as a chronometer in this case, Allende CAIs appear to have undergone some alteration prior to formation of the Allende parent body. Fluffy Type A CAIs may be more generally characterized by early (nebular?) alteration relative to

type B and compact Type A CAIs; more data are required to confirm this possibility.

**References:** [1] Hutcheon I. D. and Newton R. C. (1981) *LPS XII*, 491-493. [2] Wark D. A. (1981) *LPS XXII*, 1145-1147. [3] Davis A. M. et al. (1994) *LPS XXV*, 315-316. [4] Fagan T.J. et al. (2005) *LPS XXXVI*, #1820. [5] MacPherson G.J. et al. (1995) *Meteoritics* 30, 365-386. [6] Podosek F.A. et al. (1991) *GCA* 55, 1083-1110.

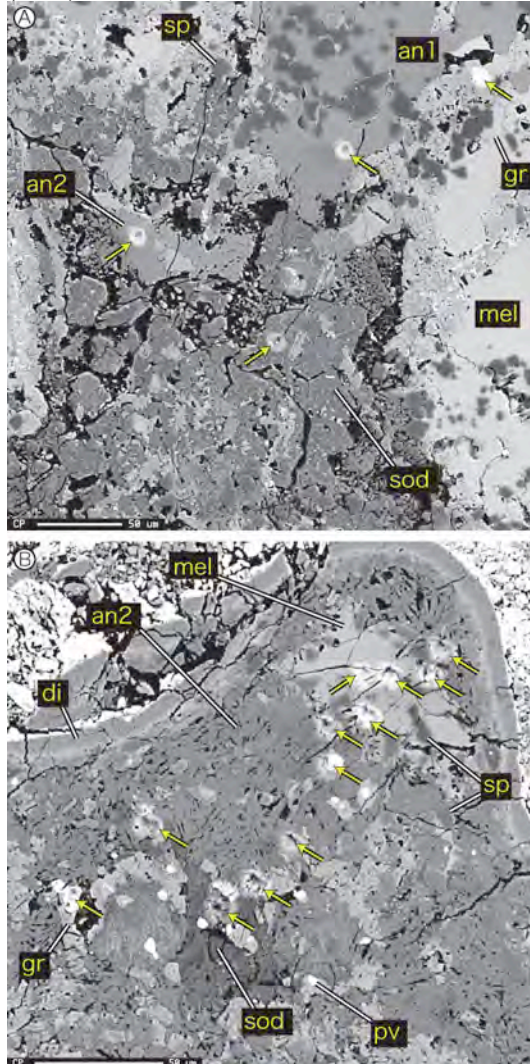


Figure 1. Back-scattered electron images (BEI) showing mineralogy and textures of altered domains in Allende CAIs. The BEI are overlain on secondary electron images to highlight SIMS craters (arrows). (A) Feldspathoid-rich patch in the interior of type B2 CAI 4022-1. (B) Secondary anorthite-rich domain near the margin of a melilite nodule of fluffy type A CAI 3529-47-1. Abbreviations: an1 = primary anorthite; an2 = secondary anorthite; di = diopside; gr = grossular; mel = melilite; pv = perovskite; sod = sodalite; sp = spinel.

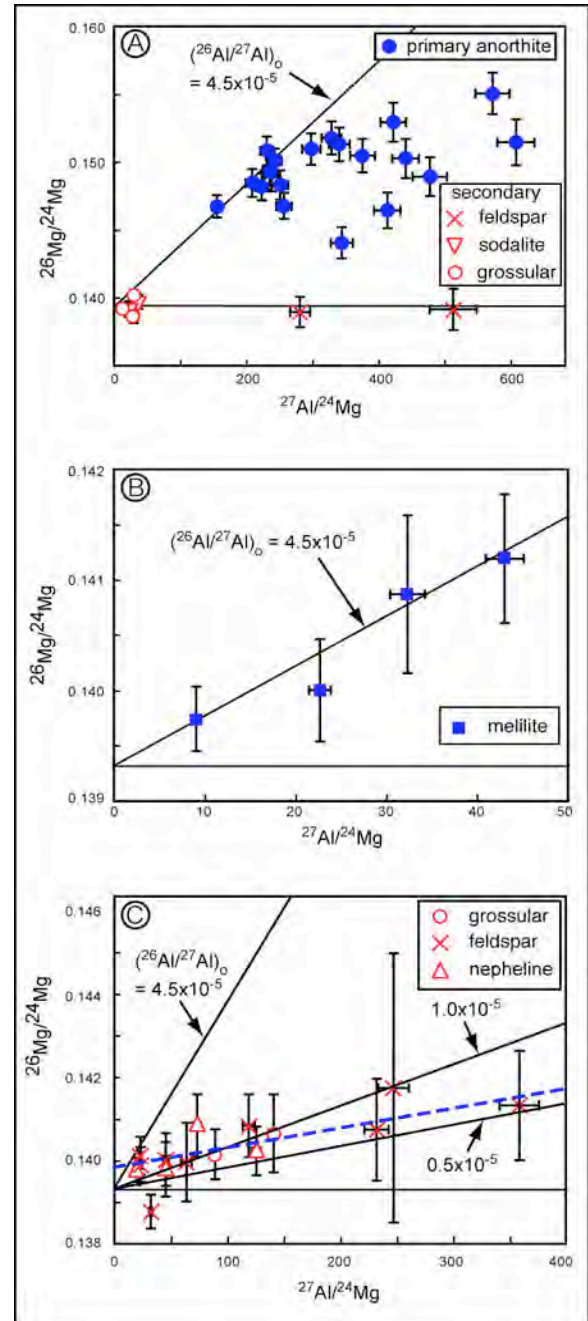


Figure 2. Al-Mg isotopic results from Allende CAIs 4022-1 (A) and 3529-47-1 (B, C). Error bars show  $2\sigma$  analytical error. Two analyses with normal  $^{26}\text{Mg}/^{24}\text{Mg}$  have Al/Mg too high to be plotted in (A) and (C): primary anorthite in 4022-1 ( $^{27}\text{Al}/^{24}\text{Mg} \sim 1050$ ) and sodalite in 3529-47-1 ( $^{27}\text{Al}/^{24}\text{Mg} \sim 2200$ ). Lines showing initial Al isotopic ratios are not fits to the data; rather, they are shown for reference. Blue dashed line in C is a fit to data excluding analyses of sodalite with  $^{27}\text{Al}/^{24}\text{Mg} \sim 2200$  (not plotted) and feldspar with  $^{27}\text{Al}/^{24}\text{Mg} = 32$ ,  $^{26}\text{Mg}/^{24}\text{Mg} = 0.1388$  (plotted).